

1S_0 proton superfluidity in neutron star matter: Impact of bulk properties

Tomonori Tanigawa*

*Japan Society for the Promotion of Science, Chiyoda-ku, Tokyo 102-8471, Japan and
Advanced Science Research Center, Japan Atomic Energy Research Institute, Tokai, Ibaraki 319-1195, Japan*

Masayuki Matsuzaki†

Department of Physics, Fukuoka University of Education, Munakata, Fukuoka 811-4192, Japan

Satoshi Chiba‡

Advanced Science Research Center, Japan Atomic Energy Research Institute, Tokai, Ibaraki 319-1195, Japan

(Dated: March 30, 2022)

We study the 1S_0 proton pairing gap in neutron star matter putting emphasis on influence of the Dirac effective mass and the proton fraction on the gap within the relativistic Hartree-Bogoliubov model. The gap equation is solved using the Bonn- B potential as a particle-particle channel interaction. It is found that the maximal pairing gap Δ_{\max} is 1–2 MeV, which has a strong correlation with the Dirac effective mass. Hence we suggest that it serves as a guide to narrow down parameter sets of the relativistic effective field theory. Furthermore, the more slowly protons increase with density in the core region of neutron stars, the wider the superfluid range and the slightly lower the peak of the gap become.

PACS numbers: 26.60.+c, 97.60.Jd, 21.60.-n

I. INTRODUCTION

Superfluidity in neutron star matter is one of the hot issues in nuclear astrophysics since superfluidity plays a key role in affecting the cooling of neutron stars [1]. Unlike the 1S_0 neutron pairing, the 1S_0 proton pairing occurs in dense matter with supranuclear density, where its properties are not much known. Such a region is highly relevant to the URCA processes that control cooling of neutron stars.

In neutron stars, several types of baryon pairing are believed to appear. In the inner crust region, neutrons will form the 1S_0 pairs [2, 3, 4]. At the corresponding baryon density $10^{-3}\rho_0 \lesssim \rho_B \lesssim 0.7\rho_0$, where $\rho_0 \simeq 0.15 \text{ fm}^{-3}$ is the saturation density of symmetric nuclear matter, the 1S_0 partial wave of the nucleon-nucleon (NN) interaction is attractive. This attraction helps neutrons pair up through the well-known BCS mechanism. In the core region $\rho_B \gtrsim 0.7\rho_0$, the 3P_2 neutron pairing may also appear since the 3P_2 partial wave of the NN interaction becomes attractive enough [2, 5]. In contrast, the 1S_0 partial wave would become repulsive there so that the neutrons would cease to pair in the 1S_0 state. Instead, the 1S_0 proton pairs are predicted to appear owing to its fraction smaller than neutrons [2, 4]. At much more higher baryon density $\rho_B \gtrsim 2\rho_0$, various hyperons may emerge; some kinds of them possibly form pairs in the same way as nucleons do [6, 7, 8]. We, however, stay

on a picture of neutron stars without hyperons in the present study.

The size of the nuclear pairing gap in dense matter is controversial since many uncertainties remain regarding NN interactions in dense medium, methods of approximation, sparsity of experimental data under extreme conditions, and so on. From the perspective of the present status of immaturity, a great deal of study with diversity is absolutely necessary. In the meantime, many studies of neutron stars have been performed using various frameworks so far. Recently, relativistic models are attracting attention in researches on neutron stars since they are suitable to describe the stars in compliance with the special relativity [9]. Most often used among them is the relativistic mean field (RMF) model, particularly owing to its economical way of description. Hence we choose the extended model of it, the relativistic Hartree-Bogoliubov (RHB) model as the framework of the present study.

The primary aim of this paper is to elucidate effects of bulk properties on the 1S_0 proton pairing correlation in neutron star matter (consisting of n , p , e^- , and μ^-) using the RHB model with capability of handling the pairing correlation. Here we show importance of environmental properties of dense matter that surrounds Cooper pairs of protons (the pairs themselves are of course a part of the environment). In particular, the Dirac effective mass of nucleons and the proton fraction are considered as accompanying quantities of great importance since the bulk properties are influential on superfluidity in neutron stars. Therefore we aim to address the bulk properties of neutron star matter and its superfluidity on the same footing within the RHB model.

The present study covers the two aforementioned quantities: The Dirac effective mass has an effect on the pairing correlation via the density of states. The symmetry

*Mailing address: Japan Atomic Energy Research Institute, Tokai, Ibaraki 319-1195, Japan; Email address: tanigawa@tiger02.tokai.jaeri.go.jp

†Email address: matsuzaki@fukuoka-edu.ac.jp

‡Email address: sachiba@popsvr.tokai.jaeri.go.jp

energy coefficient controls the proton fraction in neutron star matter, especially its density dependence. Needless to say, they connect with the equation of state (EOS) of dense matter; it is strongly related to properties of neutron stars, such as their internal structure, mass, radius, and so on. These macroscopic properties of neutron stars set stringent microscopic requirements for constituents; hence the pairing correlation is no exception. In this study, we use two distinct RMF models with two distinct parameter sets for each to compose neutron star matter; thereby we have four distinct EOSs here. Two of them are for a comparison of the effect of the Dirac effective mass, the other two are for a comparison of the effect of the proton fraction.

This paper is organized as follows. In Sec. II, model Lagrangians and the gap equation for the 1S_0 proton superfluidity are illustrated. In Sec. III, results of the pairing properties in neutron star matter are presented. Section IV contains our summary and conclusions.

II. MODELS

As is well known nowadays, the RMF model Lagrangian with nonlinear cubic, quartic terms of σ bosons, and a quartic one of ω mesons has achieved remarkable successes in studies on nuclear/hadronic physics. This type of Lagrangian was initiated by Bodmer [10] and has matured steadily [11, 12]. A parameter set is determined so as to reproduce the saturation properties of symmetric nuclear matter and ground-state properties of typical finite nuclei. A prominent feature of the model is that scalar and vector self-energies (or Hartree fields) follow the density-dependence of those obtained by the Dirac-Brueckner-Hartree-Fock (DBHF) approach even in moderately supranuclear density. Hence, the model is considered to have the capability to deal with neutron star matter at such density. This model Lagrangian is of the form

$$\begin{aligned} \mathcal{L} = & \bar{\psi}[i\gamma_\mu\partial^\mu - (M + g_\sigma\sigma) - g_\omega\gamma_\mu\omega^\mu - g_\rho\gamma_\mu\boldsymbol{\tau} \cdot \mathbf{b}^\mu]\psi \\ & + \frac{1}{2}(\partial_\mu\sigma)(\partial^\mu\sigma) - \frac{1}{2}m_\sigma^2\sigma^2 - \frac{g_2}{3}\sigma^3 - \frac{g_3}{4}\sigma^4 \\ & - \frac{1}{4}\Omega_{\mu\nu}\Omega^{\mu\nu} + \frac{1}{2}m_\omega^2\omega_\mu\omega^\mu + \frac{c_3}{4}(\omega_\mu\omega^\mu)^2 \\ & - \frac{1}{4}\mathbf{B}_{\mu\nu} \cdot \mathbf{B}^{\mu\nu} + \frac{1}{2}m_\rho^2\mathbf{b}_\mu \cdot \mathbf{b}^\mu, \end{aligned} \quad (1)$$

where $\Omega_{\mu\nu} = \partial_\mu\omega_\nu - \partial_\nu\omega_\mu$ and $\mathbf{B}_{\mu\nu} = \partial_\mu\mathbf{b}_\nu - \partial_\nu\mathbf{b}_\mu$. The symbols ψ , σ , ω_μ , \mathbf{b}_μ , M , m_σ , m_ω , and m_ρ signify the fields of nucleons, σ bosons, ω mesons, ρ mesons, the masses of nucleons, σ bosons, ω mesons, and ρ mesons, respectively. We call Eq. (1) “standard RMF Lagrangian.”

As an extension of the well-established standard RMF model, the effective field theory (EFT) [13] provides a modern aspect of the RMF model; an energy density

functional obtained from the RMF Lagrangian approximates the *exact* energy density functional of the ground state of a hadronic system in the sense of the density functional theory (DFT). Adding apt interaction terms, absent in the standard one, to the RMF functional advances it to the exact functional little by little. In this EFT-inspired approach, mesons and baryons are not taken as elementary degrees of freedom, so that a Lagrangian composed of corresponding fields is allowed to be non-renormalizable. This leads to, in principle, unrestricted inclusion of *any* terms of meson self-interactions consistent with symmetries of the underlying theory, QCD. These terms are completely absent in the standard RMF Lagrangians that respect renormalizability. Recently, Horowitz and Piekarewicz proposed an RMF Lagrangian along with concepts and methods of the EFT and the DFT. They extended the standard RMF Lagrangian with a nonlinear ω - ρ coupling particularly from the viewpoint of the symmetry energy. The new coupling paves the way to change the density dependence of the symmetry energy, and hence the proton fraction in neutron star matter. For the extended Lagrangian, the present study employs an additional interaction Lagrangian of the form [14]

$$\mathcal{L}_{\text{EFT}} = \mathcal{L} + 4g_\rho^2\mathbf{b}_\mu \cdot \mathbf{b}^\mu\Lambda_\omega g_\omega^2\omega_\nu\omega^\nu, \quad (2)$$

where Λ_ω signifies a nonlinear coupling constant. We name Eq. (2) “EFT-inspired Lagrangian.” The important thing is that the Lagrangian (2) gives the symmetry energy coefficient

$$a_{\text{sym}} = \frac{k_F^2}{6\sqrt{k_F^2 + M^{*2}}} + \frac{g_\rho^2}{3\pi^2} \frac{k_F^3}{m_\rho^{*2}}. \quad (3)$$

The symbol m_ρ^* denotes the effective mass of ρ mesons

$$m_\rho^{*2} = m_\rho^2 + 8g_\rho^2\Lambda_\omega g_\omega^2\langle\omega_0\rangle^2, \quad (4)$$

where $\langle\mathcal{O}\rangle$ represents an expectation value of a field \mathcal{O} for the ground state of the system. In this study, we pick out the NL3-hp and Z271 parameter sets [14, 15]; each set gives the lower or upper limit of commonly accepted range of the effective nucleon mass in symmetric nuclear matter at ρ_0 , $M^* \simeq (0.6\text{--}0.8)M$. Most RMF parameter sets yield the mass within this range. Note that we rename the NL3 set by Horowitz and Piekarewicz in Ref. [14] here because of their slight modification of the well-known NL3 parameter set [16]. We will also mention the TM1 parameter set [12] for the standard RMF Lagrangian in addition to the above two sets. Table I shows the parameter sets.

In neutron star matter composed by the models, we solve the gap equation for the 1S_0 proton pairing correlation at zero temperature using the Bonn- B potential [17] as a particle-particle (p - p) channel interaction \bar{v} ,

$$\begin{aligned} \Delta(p) = & -\frac{1}{8\pi^2} \int_0^\infty \frac{\Delta(k)}{\sqrt{(E_k - E_{k_F})^2 + \Delta^2(k)}} \\ & \times \bar{v}(p, k) k^2 dk, \end{aligned} \quad (5)$$

TABLE I: Parameter sets used in the present study. We fix the bare nucleon mass $M = 939.0$ MeV and the ρ meson mass $m_\rho = 763.0$ MeV, except for TM1 where $M = 938.0$ MeV and $m_\rho = 770.0$ MeV are used.

Parameter set	m_σ [MeV]	m_ω [MeV]	g_σ	g_ω	g_2 [fm $^{-1}$]	g_3	c_3	g_ρ
NL3-hp ($\Lambda_\omega = 0$)	508.194	782.5	10.217	12.868	-10.431	-28.885	0	4.461
NL3-hp ($\Lambda_\omega = 0.025$)	508.194	782.5	10.217	12.868	-10.431	-28.885	0	5.376
Z271 ($\Lambda_\omega = 0$)	505.0	783.0	7.031	8.4065	-5.4345	-63.691	49.94	4.749
Z271 ($\Lambda_\omega = 0.040$)	505.0	783.0	7.031	8.4065	-5.4345	-63.691	49.94	5.008
TM1 ($\Lambda_\omega = 0$)	511.198	783.0	10.0289	12.6139	-7.2325	0.6183	71.3075	4.6322

where $E_k = \sqrt{k^2 + M^{*2}} + g_\omega \langle \omega_0 \rangle + g_\rho \langle b_0^{(3)} \rangle$. The p - p channel interaction between protons $\bar{v}(p, k)$ is obtained through angular integration with respect to the angle between linear momenta \mathbf{p} and \mathbf{k} . This serves as a process of projecting out the S -wave component of the interaction. Its original form is nothing but the antisymmetrized matrix element of the employed interaction V , which is defined by

$$\bar{v}(\mathbf{p}, \mathbf{k}) = \langle \mathbf{p}s', \widetilde{\mathbf{p}s'} | V | \mathbf{k}s, \widetilde{\mathbf{k}s} \rangle - \langle \mathbf{p}s', \widetilde{\mathbf{p}s'} | V | \widetilde{\mathbf{k}s}, \mathbf{k}s \rangle, \quad (6)$$

where a tilde over its argument denotes time reversal. We use the lowest approximation as to the p - p channel interaction to study exclusively the effect of the bulk properties on superfluidity. It is, however, known that the polarization effects bring about significant reduction of the gap within nonrelativistic frameworks [18, 19].

The models employed here should be regarded as hybrid models because we use different interactions in the particle-hole (p - h) and the particle-particle channel. This prevents ambiguity in choosing the pairing interaction. Thus we concentrate on the study of the effect of the Dirac effective mass and the proton fraction on the proton superfluidity.

III. RESULTS AND DISCUSSION

To begin with, we calculate the 1S_0 pairing gaps and the Dirac effective masses of protons *without* the isovector nonlinear coupling. The results are shown in Fig. 1, which apparently shows that the gaps strongly depend on the Dirac effective masses. The smaller the mass is, the smaller the pairing gap is. The NL3-hp set makes symmetric nuclear matter saturated with the Dirac effective mass of $0.59M$, while the Z271 set does with that of $0.80M$. According to Ref. [15], both sets give similar properties of typical finite nuclei and low-mass neutron stars on the one hand, different properties of typical neutron stars of mass $1.4M_\odot$ follow from the sets on the other hand. For comparison, we also present the result of the TM1 set in Fig. 1 with the light gray curves. The effective mass obtained by the TM1 set lies in between those by the other two sets, so does the pairing gap; it is consistent with the above statement as well. In view of the pairing correlation in neutron star matter, using the different p - h interactions and the same p - p interaction

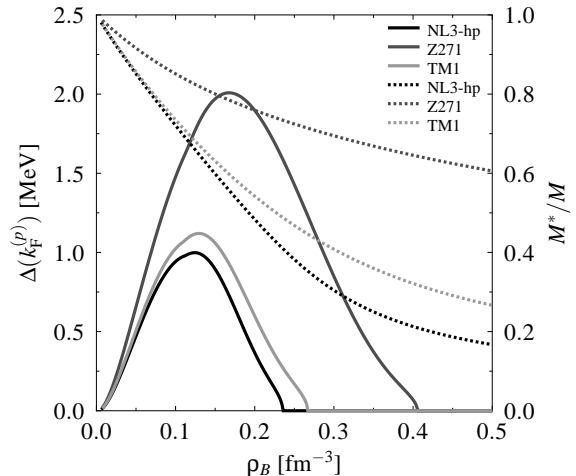


FIG. 1: 1S_0 proton pairing gaps (left scale, solid curves) and Dirac effective masses (right scale, dashed curves) as functions of baryon density in neutron star matter using the standard RHB model with the NL3-hp, Z271 [14], and TM1 [12] parameter sets.

gives the significant difference shown in Fig. 1. Hence, this suggests that we can use the strong correlation as a guide to narrow down the parameter sets favorable for a calculation such as the present study.

Next, we show the proton fractions $Y_p = \rho_p/\rho_B$ in Fig. 2 for the variations of Lagrangian. The solid black curve denotes the proton fraction obtained by the NL3-hp set, the solid gray curve by the Z271 set, both *without* the new nonlinear coupling. Their characteristic is the large proton fraction, which is the typical result obtained from the standard RMF Lagrangian. The result obtained by the TM1 set is similar to the one by the NL3-hp set without the coupling (and hence is omitted hereafter). In contrast, using finite Λ_ω , namely, the EFT-inspired RMF Lagrangian, we have obtained smaller proton fractions at densities corresponding to the core region of neutron stars, $\rho_B \gtrsim 0.1$ fm $^{-3}$, than using $\Lambda_\omega = 0$; these fractions are drawn with dashed curves in Fig. 2. As the original intent of this kind of Lagrangian [14], it yields gentle increase of the fraction at these relevant densities owing to the symmetry energy adjustable via the isovector nonlinear coupling Λ_ω indicated by Eqs. (3) and (4). Not shown are curves of the proton fraction that lie in between the two extreme conditions $\Lambda_\omega = 0$ and 0.025 (0.040) for the

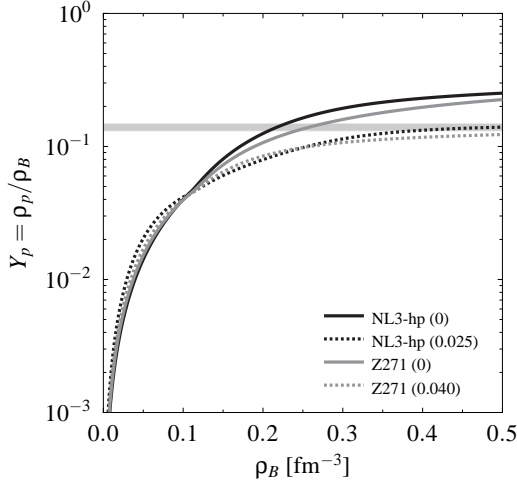


FIG. 2: Proton fractions of the four distinct models of neutron star matter as functions of baryon density. The thin region hatched in gray represents a threshold of the proton fraction for the direct URCA process, about 13–15 %. The number in parenthesis in the legend indicates the value of Λ_ω .

NL3-hp (Z271) set, when it is varied between them. To wind up the account of Fig. 2, we should note how each curve of the proton fraction depends on baryon density, with its influence on the pairing correlation in mind.

To offer more direct information on the 1S_0 proton pairing gaps at the proton Fermi surface and their relation to the proton fractions, we present the gaps as functions of the proton Fermi momentum in Fig. 3. An apparent difference between the gaps obtained with the NL3-hp and Z271 sets stems, again, from the difference of the Dirac effective masses between the sets, as shown in Fig. 1. In addition, the two curves for each parameter set with and without Λ_ω reflect the increase rate of the proton fraction as functions of baryon density (see Fig. 2). Comparing the property of protons at the same Fermi momentum explains further details about that: With Λ_ω , where the rate is moderate at the relevant densities, the proton Cooper pairs are immersed in denser background than those without Λ_ω , where the rate is rapid. Meanwhile, the higher the baryon density is, the smaller the Dirac effective mass of protons is. We thus obtain the smaller pairing gaps at the same Fermi surface for the parameter sets with Λ_ω , namely, for the EFT-inspired Lagrangian.

We compare the pairing gaps as functions of baryon density obtained with and without the isovector nonlinear coupling Λ_ω in Fig. 4. Since the density dependence of the Dirac effective masses obtained from the respective parameter sets is almost the same for any values of Λ_ω , the obtained gaps reflect the respective proton fractions presented in Fig. 2. As a whole, the pairing gaps survive in higher density region for the EFT-inspired Lagrangian with finite Λ_ω , and have lower peaks than for the standard Lagrangian with $\Lambda_\omega = 0$. Figures 2 and 4 give indications as follows.

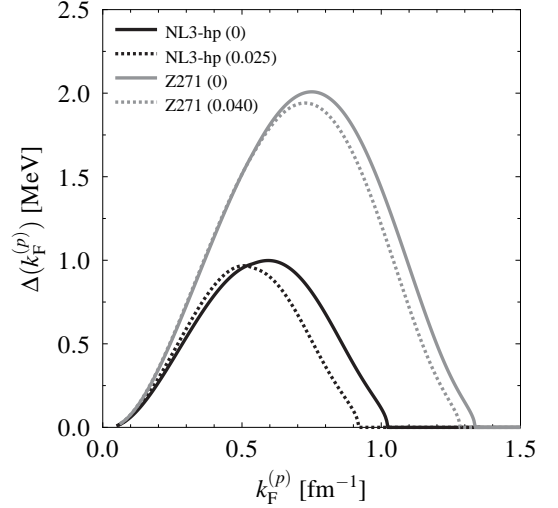


FIG. 3: 1S_0 proton pairing gaps as functions of the proton Fermi momentum in neutron star matter using the RHB models with the NL3-hp and Z271 parameter sets with and without Λ_ω . The legend is the same as in Fig. 2.

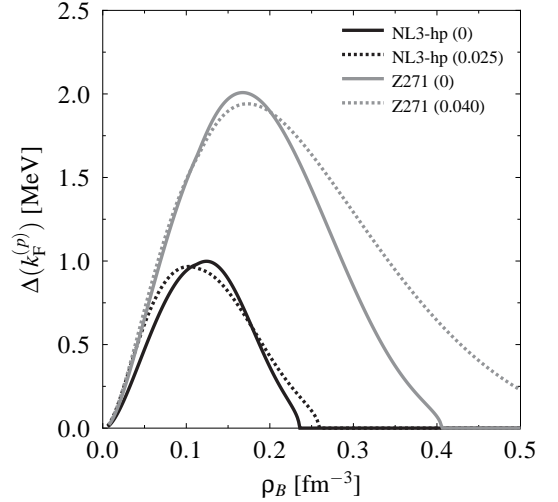


FIG. 4: 1S_0 proton pairing gaps as functions of baryon density in neutron star matter using the RHB models with the NL3-hp and Z271 parameter sets with and without Λ_ω . Solid curves and the legend are the same as in Figs. 1 and 2, respectively.

(1) Up to $\rho_B \simeq 0.05 \text{ fm}^{-3}$, the proton fractions are almost the same except the one of the NL3-hp set with finite Λ_ω , which is a little larger than the others (see Fig. 2). The enhancement of the gap due to the large proton fraction cancels out the smallness of the effective mass given by the NL3-hp set. Hence, the pairing gap obtained by the NL3-hp set with $\Lambda_\omega = 0.025$ is almost the same as those by the Z271 set. We note, however, that this region roughly corresponds to the inner crust of neutron stars, where the 1S_0 proton pairing is much weaker than the neutron counterpart.

(2) At $\rho_B \approx 0.1 \text{ fm}^{-3}$, as the proton fractions of the

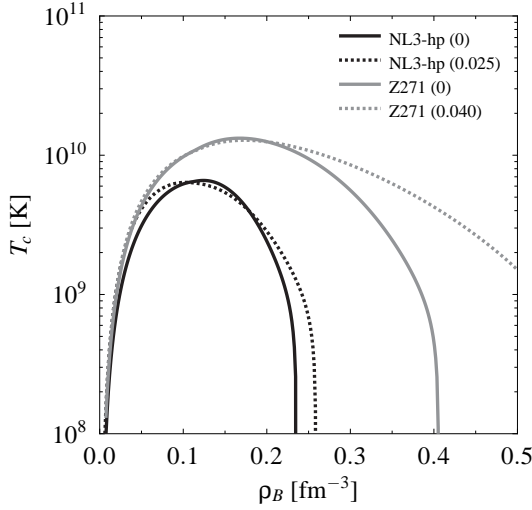


FIG. 5: Critical temperatures of 1S_0 proton superfluids as functions of baryon density in neutron star matter using the RHB models with the NL3-hp and Z271 parameter sets with and without Λ_ω . The legend is the same as in Fig. 2.

Z271 set start to deviate from each other, so do the pairing gaps obtained by the set. As to the NL3-hp set, the proton fractions for $\Lambda_\omega = 0$ and 0.025 nearly coincide there, so do the pairing gaps.

(3) For $0.1 \text{ fm}^{-3} \lesssim \rho_B \lesssim 0.2 \text{ fm}^{-3}$, the high proton fractions make the corresponding pairing gaps large. This implies that richness of protons favors the pairing correlation by taking advantage of an attractive part of the proton-proton interaction in this region.

(4) At $\rho_B \approx 0.2 \text{ fm}^{-3}$, an opposite situation to the previous case (3) is realized; namely, the high proton fractions make the corresponding pairing gaps small. This implies that richness of protons disfavors the pairing correlation by virtue of a repulsive part of the proton-proton interaction in this region. As a result of the difference between the effective masses, the pairing gap given by the Z271 set is still very large. To sum up the discussion of Fig. 4, the more gently protons multiply in the core region of neutron stars, up to the higher density superfluidity survives and the somewhat smaller the peak of the gap one obtains.

Let us here present three figures relevant to the physics of neutron stars. One is Fig. 5, which represents the density dependence of the critical temperatures of the superfluids. The critical temperatures T_c are obtained by the universal relation for a weak-coupling BCS superconductor at $T = 0$ K, $k_B T_c = 0.57 \Delta(k_F^{(p)}; T = 0)$, where k_B is the Boltzmann constant. Since the temperature inside evolved neutron stars is about 10^8 K, Fig. 5 signifies that the superfluidity is likely to exist in the all cases considered. The other two are Figs. 6 and 7, which depict the neutrino emissivities Q and their reduction factor R by the 1S_0 proton superfluidity as functions of baryon density, drawn at the internal temperatures $T = 1.0 \times 10^8$ K and 3.0×10^8 K. We now take, for example, the nucleon

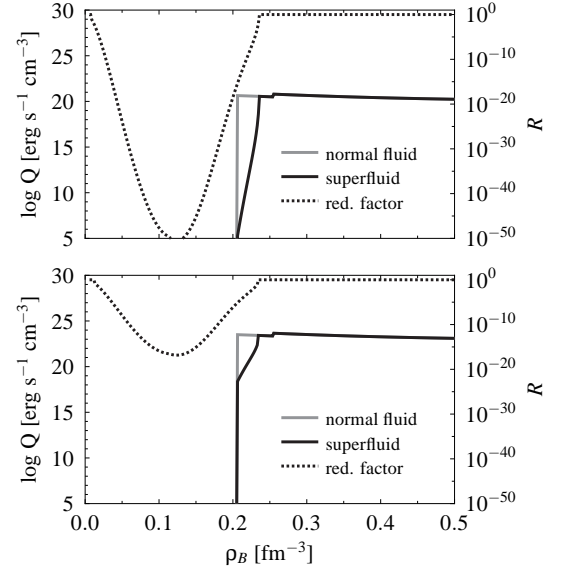


FIG. 6: Neutrino emissivities of the nucleon direct URCA process (left scale, solid curves) and the reduction factor for 1S_0 proton pairing (right scale, dashed curve) as functions of baryon density in neutron star matter for the NL3-hp parameter set without Λ_ω . Solid gray curves represent the neutrino emissivities in normal fluid. The upper panel is drawn for the internal temperature $T = 1.0 \times 10^8$ K, the lower for $T = 3.0 \times 10^8$ K.

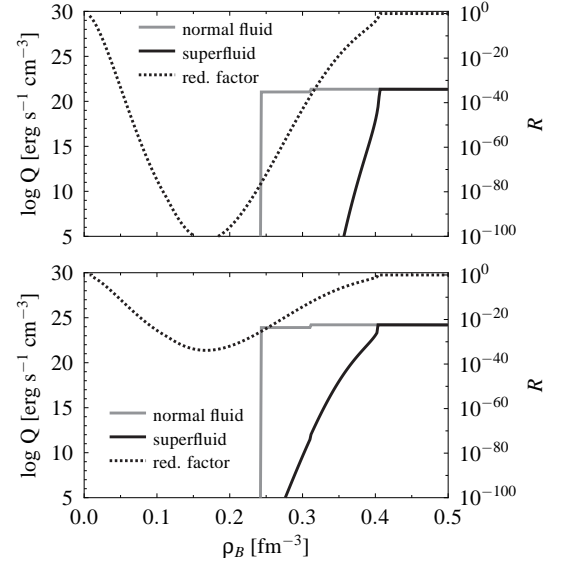


FIG. 7: Same as Fig. 6, but for the Z271 parameter set without Λ_ω . Also note that the right scales are different from those of Fig. 6.

direct URCA process as a cooling agent of neutron stars. The neutrino emissivity of the nucleon direct URCA process in normal fluid Q_0 has the following form in units of $\text{erg s}^{-1} \text{ cm}^{-3}$ [20]:

$$Q_0 = 7.55 \times 10^{30} \mu_e T_9^6 \frac{M_n^{*2} M_p^{*2}}{M^2} \theta(p_{Fe} + p_{Fp} - p_{Fn}), \quad (7)$$

where μ_e is the chemical potential of electrons (and muons due to the condition of beta equilibrium), T_9 is the temperature in units of 10^9 K, and $\theta(p_{Fe} + p_{Fp} - p_{Fn})$ is the triangle condition for particle momenta. After the appearance of muons, they also contribute to the neutrino emission so that the emissivity Q_0 just doubles, which manifests itself as the small kinks after the ignition of the process involving electrons (abrupt increase of the emissivities) in Figs. 6 and 7. It should be noted that we approximate the effective masses $M_n^* = M_p^* = M^*$ in Eq. (7): To distinguish between them in the RMF model, we must introduce isovector-scalar mesons and shortly discuss this issue later. The neutrino emissivity in superfluid is thus written as $Q = Q_0 R$, the reduction factor used here being

$$\begin{aligned} R &\simeq \exp \left[-\Delta(k_F^{(p)}; T)/k_B T \right] \\ &\simeq \exp \left[-\Delta(k_F^{(p)}; T=0)/k_B T \right] \\ &\simeq \exp \left[-1.76 T_c(k_F^{(p)})/T \right], \end{aligned} \quad (8)$$

which is the form often used in the past studies. It should be mentioned that the reduction factor of the form (8) leads to an overestimate of the suppressive effect [21, 22]. Although we have employed the pairing gaps at $T = 0$ K for a qualitative estimate in the present study, one should use the pairing gaps at finite temperatures for a quantitative study of thermal evolution of neutron stars.

As shown in Figs. 1 and 2, both the NL3-hp and the Z271 set with $\Lambda_\omega = 0$ yield the relatively large proton fraction. Meanwhile, the pairing gap for the NL3-hp set closes around the density at which the direct URCA process takes effect. Therefore, the reduction effect is not much large, which is clear for $T = 3.0 \times 10^8$ K as shown in Fig. 6. By comparison, the superfluid range for the Z271 set is wide enough to cover the density region where the direct URCA process is turned on. Hence the process is strongly suppressed by the interior proton superfluid as shown in Fig. 7. For both sets with finite Λ_ω , on the other hand, the density regions of the superfluidity and the direct URCA process do not overlap each other; the latter starts at $\rho_B = 0.442 \text{ fm}^{-3}$ with $Y_p = 0.136$ for the NL3-hp set and at $\rho_B = 1.028 \text{ fm}^{-3}$ with $Y_p = 0.141$ for the Z271 set. Thus the superfluidity is of no suppressive effect on the direct URCA process for both with finite Λ_ω .

Now we develop a brief discussion on the cooling of neutron stars relative to the above results. From the aspect of surface temperature of neutron stars, we can classify observed neutron stars into hotter and colder ones. Broadly speaking, this means that there exist two major cooling scenarios; the so-called “standard” and “nonstandard” cooling [23]. The standard cooling is dominated by the modified URCA process, which cools neutron stars slowly and thus results in hotter stars. In contrast, the nonstandard cooling includes the nucleon/hyperon direct URCA processes, via which neutron stars cool faster

and lead to colder stars, in conjunction with the suppression due to superfluidity. Concerning this classification, the pulsar PSR J0205+6449 was recently discovered in the supernova remnant 3C 58 by Murray *et al.* [24]. Slane *et al.* subsequently deduced a strong upper limit on the surface temperature [25]. They showed that the limit falls below the prediction of the standard cooling model, which suggests that PSR J0205+6449 seems to follow the nonstandard cooling scenario. In the first place, the proton fraction higher than about 13–15 % (shown by the hatched region in Fig. 2) activates the direct URCA process involving nucleons in neutron star matter with the standard RMF Lagrangian. However, our results from the Z271 set show that the proton pairing gap is large enough to suppress the process, so that the resulting cooling of neutron stars is not much effective to meet observational data of colder neutron stars. This calls for the cooling that results from hyperons or meson condensates; the latter consequently means coexistence of superfluidity and meson condensations. In the second place, using the EFT-inspired RMF Lagrangian with the Z271 set, neutron star matter is composed with the proton fraction lower than the direct URCA threshold up to $\sim 7\rho_0$. This prohibits neutron stars from cooling by the direct URCA process involving nucleons; the modified URCA process dominates their cooling instead, given the present constituent particles. In this regard, Horowitz and Piekarewicz studied the direct URCA process in detail using the EFT-inspired RMF Lagrangian with intermediate values of Λ_ω [26]. Bear in mind that we have put aside the Cooper pair breaking and formation processes [27, 28] that work as a cooling accelerator, while we have taken superfluidity into account as a cooling retardant alone: Since the neutrino emissivity of these processes sensitively depends on the density and the temperature dependence of the pairing gap, our approximate treatment at the moment does not allow us to estimate this emissivity and to determine the scenario that the pulsar follows.

Finally, we should note preceding works on the 1S_0 proton superfluidity in neutron star matter. According to them, nonrelativistic approaches and the Dirac-Brueckner-Hartree-Fock approach give similar results with the maximal pairing gap $\Delta_{\text{max}} \lesssim 1.0$ MeV and the closing density $\rho_c \sim 0.4 \text{ fm}^{-3}$ [29, 30, 31]. The discrepancy between them and our results having been exposed, with the reservation of the lowest approximation, we now need information to narrow down further RMF parameter sets for the purpose like the present study. In this context, extracting the EOS from direct observation of the stars and experiments of neutron-rich nuclei is indispensable.

IV. SUMMARY AND CONCLUSIONS

We have investigated the 1S_0 proton pairing in neutron star matter using the relativistic Hartree-Bogoliubov

model. Since proton Cooper pairs reside in extremely dense surroundings inside neutron stars, special care should be taken of the effects of the bulk properties, as well as pairing interactions and levels of the approximation. Therefore, we have studied the effects on the pairing correlation using the lowest approximation with respect to the pairing interaction. We summarize and conclude the following: First, using the standard RMF parameter, we have obtained that the maximal pairing gap is about 1–2 MeV, dependent on the parameter sets used, which is comparable or larger than the values obtained in the preceding studies. This clearly shows the strong correlation between the effective mass of nucleons and the pairing gap, which was also concluded within nonrelativistic models. Although the relativistic model tends to have a smaller effective mass of nucleons (the Dirac effective mass) than those in nonrelativistic models, the value of the maximal gap is not much small against general expectations. Second, we have studied the problem also using the extended Lagrangian proposed in line with a concept of the EFT by Horowitz and Piekarewicz [14]. The proton fraction obtained can be controlled by the additionally introduced parameter Λ_ω . We have found that the more slowly protons increase with density in the core region of neutron stars, the wider the superfluid range and the slightly lower the peak of the gap become.

In this study, we have ruled out direct effects of the bulk properties on the p - p channel interaction: For in-

stance, self-consistent (or in-medium) Dirac spinors in the p - p channel are not used here though they probably affect properties of the pairing correlation at high density [8]. Furthermore, we have included no isovector-scalar meson, which may play important roles in high-density and isovector physics through larger effective mass of protons than that of neutrons [32]. In general, the isovector-scalar meson increases protons in the high-density region, which is an effect opposite to that of the EFT-inspired Lagrangian employed here. Last but not least, having clarified the effects of the bulk properties on superfluidity by solving the gap equation at zero temperature, we are prepared for solving it at finite temperatures. It will be mandatory to consider these issues. With attention to the bulk properties of neutron star matter, a study of baryon superfluidity therein and accompanying neutrino emissivities is in progress.

Acknowledgments

One of us (T.T.) is grateful to the Japan Society for the Promotion of Science for research support and the members of the research group for manybody theory of hadron systems at the Japan Atomic Energy Research Institute (JAERI) for fruitful discussions.

-
- [1] T. Kunihiro, T. Muto, T. Takatsuka, R. Tamagaki, and T. Tatsumi, *Prog. Theor. Phys. Suppl.* **112**, 1 (1993).
 - [2] T. Takatsuka and R. Tamagaki, *Prog. Theor. Phys. Suppl.* **112**, 27 (1993).
 - [3] J. Wambach, T. L. Ainsworth, and D. Pines, *Nucl. Phys.* **A555**, 128 (1993).
 - [4] J. M. C. Chen, J. W. Clark, R. D. Davé, and V. V. Khodel, *Nucl. Phys.* **A555**, 59 (1993).
 - [5] Ø. Elgarøy, L. Engvik, M. Hjorth-Jensen, and E. Osnes, *Nucl. Phys.* **A607**, 425 (1996).
 - [6] S. Balberg and N. Barnea, *Phys. Rev. C* **57**, 409 (1998).
 - [7] T. Takatsuka and R. Tamagaki, *Prog. Theor. Phys.* **102**, 1043 (1999).
 - [8] T. Tanigawa, M. Matsuzaki, and S. Chiba, *Phys. Rev. C* **68**, 015801 (2003).
 - [9] N. K. Glendenning, *Compact Stars* (Springer-Verlag, New York, 2000), 2nd ed.
 - [10] A. R. Bodmer, *Nucl. Phys.* **A526**, 703 (1991).
 - [11] S. Gmuca, *Z. Phys.* **A342**, 387 (1992).
 - [12] Y. Sugahara and H. Toki, *Nucl. Phys.* **A579**, 557 (1994).
 - [13] B. D. Serot and J. D. Walecka, *Int. J. Mod. Phys.* **E6**, 515 (1997).
 - [14] C. J. Horowitz and J. Piekarewicz, *Phys. Rev. Lett.* **86**, 5647 (2001).
 - [15] J. Carriere, C. J. Horowitz, and J. Piekarewicz, *Astrophys. J.* **593**, 463 (2003).
 - [16] G. A. Lalazissis, J. König, and P. Ring, *Phys. Rev. C* **55**, 540 (1997).
 - [17] R. Machleidt, *Adv. Nucl. Phys.* **19**, 189 (1989).
 - [18] T. L. Ainsworth, J. Wambach, and D. Pines, *Phys. Lett.* **B222**, 173 (1989).
 - [19] H.-J. Schulze, J. Cugnon, A. Lejeune, M. Baldo, and U. Lombardo, *Phys. Lett.* **B375**, 1 (1996).
 - [20] James M. Lattimer, C. J. Pethick, Madappa Prakash, and Pawel Haensel, *Phys. Rev. Lett.* **66**, 2701 (1991).
 - [21] D. Yakovlev, A. Kaminker, O. Gnedin, and P. Haensel, *Phys. Rep.* **354**, 1 (2001).
 - [22] T. Takatsuka and R. Tamagaki, *Prog. Theor. Phys.* **112**, 37 (2004).
 - [23] S. Tsuruta, *Phys. Rep.* **292**, 1 (1998).
 - [24] S. S. Murray, P. O. Slane, F. D. Seward, and S. M. Ransom, *Astrophys. J.* **568**, 226 (2002).
 - [25] P. O. Slane, D. J. Helfand, and S. S. Murray, *Astrophys. J.* **571**, L45 (2002).
 - [26] C. J. Horowitz and J. Piekarewicz, *Phys. Rev. C* **66**, 055803 (2002).
 - [27] E. Flowers, M. Ruderman, and P. Sutherland, *Astrophys. J.* **205**, 541 (1976).
 - [28] D. N. Voskresensky and A. V. Senatorov, *Sov. J. Nucl. Phys.* **45**, 411 (1987).
 - [29] T. Takatsuka and R. Tamagaki, *Prog. Theor. Phys.* **97**, 345 (1997).
 - [30] Ø. Elgarøy, L. Engvik, M. Hjorth-Jensen, and E. Osnes, *Nucl. Phys.* **A604**, 466 (1996).
 - [31] Ø. Elgarøy, L. Engvik, M. Hjorth-Jensen, and E. Osnes, *Phys. Rev. Lett.* **77**, 1428 (1996).
 - [32] S. Kubis and M. Kutschera, *Phys. Lett.* **B399**, 191 (1997).